

# Length Variation of Toothed Belt during Exploitation

Blaza Stojanović\* – Nenad Miloradović – Nenad Marjanović – Mirko Blagojević – Lozica Ivanović  
University of Kragujevac, Faculty of Mechanical Engineering, Kragujevac, Serbia

*Timing belt drives are a relatively new concept in power transmission, accepted nowadays in all areas of industry. Teeth, equally spaced on the inner side of timing belts, come into contact with the belt pulley's teeth through their grooves. By this meshing, a connection between the belt and the belt pulley is achieved and torque is transmitted.*

*This paper reviews basic tribomechanical systems in timing belt drives, focusing on the analysis of the tribomechanical system "belt's teeth - belt pulley's teeth". In addition, analysis of pitch variation and belt's length variation during testing is conducted. Friction is the main cause of wear of the flanks of the belt's teeth, which leads to an increase of pitch. Testing of the timing belt was conducted on a specially designed test bench and showed that the belt's elongation is especially distinct in a period of running in.*

©2011 Journal of Mechanical Engineering. All rights reserved.

**Keywords:** timing belt drives, belt pitch, friction, wear, tribology, tribomechanical systems

## 0 INTRODUCTION

A timing belt drive is a relatively young drive designed by Case in 1946 [1]. It was a rubber belt with trapezoidal teeth profile used as a transmitter on a sewing machine. Despite the advantages in operation, timing belt drives have just recently gained large application. It was not until the application of timing belts as IC engine's camshaft drive that usefulness of their application became obvious. The intensification of design demands in terms of an increased service life and a decreased construction mass have initiated the appearance of a large number of tests of timing belt drives [2] and [3].

Gerbert et al. [4] formed the first model of a timing belt and conducted a detailed analysis of forces acting on the belt teeth. They introduced friction force into the analysis of load distribution. Further steps in analysis of these transmitters were achieved by testing of their tractive characteristics [5], by analysing load distribution and by pretension of the timing belt [6] and [7]. Kido et al. [8] presented the first analysis of load distribution using the finite element method. Soon afterwards, the finite element method was beginning to be increasingly more introduced in the analysis of timing belt drives. Karolev and Gold [9] presented a new, changed form of the timing belt model. The analysis of load distribution takes into account the friction force and belt deformation and tests are conducted under variable torque.

Considering an increasingly more frequent use of timing belt drives, but also their limited service life, the analysis of friction and wear became more and more significant in the late 1990's. Dalgarno, Childs et al. [10] to [15] introduced new models of timing belts, taking into account the friction force between belt's teeth and belt pulley, together with friction force analysed until then only between belt pulley's teeth apexes and the belt's groove. Dalgarno et al. gave detailed analyses of meshing and tribological processes on contact surfaces.

Introduction of friction force into a new model of belt [16] and [17] and belt's model with mass [18] and [19] showed that the results obtained by application of numerical methods completely coincide with experimental results, regarding load distribution. Paper [21] presents the analysis of deformation state through a model developed by application of finite element method. Papers [22] to [23] demonstrate the modelling of friction induced noise of timing belt drives.

The retrospective of the existing tests of timing belt drives is mostly related to analyses of meshing and load distribution, both analytical and numerical. The aim of this review is to identify basic tribomechanical systems in timing belt drive and analyze them. Wear that leads to an increase of pitch and elongation of the belt appears to be a direct consequence of friction on the flanks of the belt and of the belt pulley. Elongation of the belt induces changes in kinematics of coupling and

increased friction that brings about larger power losses, that is reduction of the efficiency of the drive.

## 1 TRIBOMECHANICAL SYSTEM IN TIMING BELT DRIVES

The largest amount of motion and power is transferred by shape, while only a small amount is transferred by friction. The influence of friction should not be neglected. Appearance of friction in timing belt drives and its consequences have not been thoroughly explained. In contrast to other transmissions of power and motion (gears, chain drives, cardanic transmissions, etc.) in which friction mostly occurs in the contact of the two metal surfaces, in timing belt drives, there are one metal and one non-metal surface. The timing belt pulley of the tested timing belt drive is made of C45 steel (WNr 1.0503) with the initial teeth roughness of  $R_a = 1.6 \mu\text{m}$ . The belt's material is rubber whose initial teeth roughness depends on measurement point (apex, flank or groove), i.e.  $R_a = 9$  to  $12.5 \mu\text{m}$ .

The basic tribomechanical systems in the timing belt drives are (Fig. 1) [24]:

1. belt's tooth – belt pulley's tooth,
2. belt's face – flange,
3. the belt groove – apex of the belt pulley's tooth.

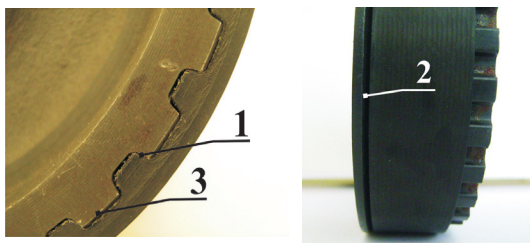


Fig. 1. Timing belt drive and basic tribomechanical systems

Types of motion that occur in these tribomechanical systems are given in Table 1.

The flank of the belt's teeth makes contact with the flank of the belt pulley's teeth, after entering the meshing. In addition, the inner surface of the belt groove and the outer surface of the belt pulley and, from time to time, the front surface of the belt pulley with the flange ring, are in contact.

Table 1. Tribomechanical systems and types of motion in timing belt drives

Tribomechanical system	Type of motion
belt's tooth – belt pulley's tooth	- impact - sliding - rolling
belt's face - flange	- impact - sliding
the belt groove – apex of the belt pulley's tooth	- sliding - rolling

The belt's tooth enters the meshing with the drive belt pulley, maximally strained due to previous tension. While entering the meshing, the belt tooth's apex contacts the flank of the belt pulley's tooth. At that moment, a line contact occurs, i.e. pure roll occurs. Due to the interference, the belt's tooth cuts into the flank of the belt pulley's tooth. Due to elastic properties of the belt and the large stiffness of the belt pulley, deformation of the belt's tooth occurs (Fig. 2, position 4). The usual initial assumption is that the stiffness of the belt pulley's is indefinitely large (rigid body) compared to the belt's stiffness [4], [9], [10], [15], [17]. Deformation of the belt's tooth grows, while, at the same time, the contact surface between the belt and the belt pulley increases. The contact point between the belt's tooth and the belt pulley tooth moves from the belt pulley's tooth apex towards its root.

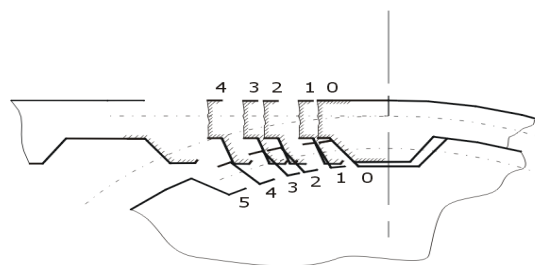


Fig. 2. Layout of belt's teeth entering the meshing with the teeth of the drive belt pulley

Maximal tooth deformation takes place in position 2 (Fig. 2). The reduction of deformations occurs due to action of internal stresses and turning of the belt and the belt pulley. Full coincidence of the flanks of the belt's teeth and the belt pulley's teeth occurs in position 1 (Fig. 2). Now, contact over surface occurs. Relative sliding

of their flanks, with appearance of the friction force, follows the process of belt's teeth entering the meshing with the belt pulley. The value of normal force varies according to parabolic law, which leads to variation of the friction force. The greatest values of normal force and friction force are at the teeth's roots.

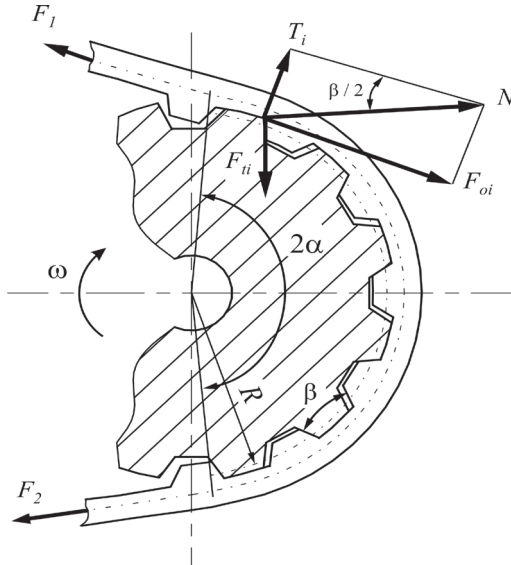


Fig. 3. Friction force at the flanks of the belt's tooth

Value of the friction force increases with the increase of the length of the sliding path and achieves its greatest value at the root of the belt's tooth (Fig. 3). At the same time, the action point of the resultant component of normal force moves from the tooth's apex towards its root. The normal force changes according to parabolic law [25]:

$$N_i = -\frac{N_{\max}}{l_t^2} \cdot (l - l_t)^2 + N_{\max}, \quad (1)$$

where  $N_{\max}$  is maximal value of normal force ( $N_{\max} \approx 1.5 F_o / z_{01}$ ) and  $l_t$  is the length of friction path.

The friction force occurs at the flank of the belt's tooth and its value is determined according to the following Eq. (2):

$$F_{t_i} = N_i \times \mu = \frac{F_{oi} \times \mu}{\cos(\beta / 2)}, \quad (2)$$

where  $N_i$  is normal force acting on the belt's tooth,  $\mu$  is the friction coefficient,  $F_{oi}$  is circumferential

force acting on the belt's tooth and  $\beta$  is the angle of the belt's profile.

## 2 TESTING OF TIMING BELT DRIVE

Testing of timing belt drive was conducted on a specially designed test bench, made at the Laboratory for Mechanical Constructions and Mechanization of the Faculty of Mechanical Engineering in Kragujevac. Test bench operates on a principle of opened loop power [26].

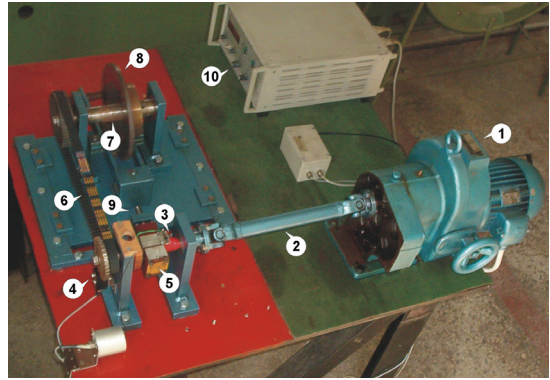


Fig. 4. Test bench for testing of timing belt

Basic elements of the test bench, Fig. 4, are:

1. drive unit (electric motor),
2. cardanic drive,
3. measuring (input) shaft,
4. input shaft's rotational speed transducer,
5. input shaft's torque transducer,
6. tested drive (timing belt drive),
7. output shaft,
8. mechanical brake,
9. tension mechanism and
10. amplifier bridge.

A toothed disc with 30 teeth on circumference is mounted on a measuring shaft. Rotational speed is read on the amplifier bridge that acquires a signal from inductive sensor HBM M1 and rotational speed pulse receiver HBM DV2556. The torque of the shaft is measured with contactless torque sensor that consists of a strain gauge, a signal transmitter HBM MT2555A and a signal receiver HBM EV2510A. Values of rotational speed and torque were displayed on a display of a digital amplifier DA24.

In order to obtain a true picture of tribological characteristics of the timing belt, measurement of roughness parameters and determination of geometrical values are conducted. Measurement of these values is conducted according to previously determined dynamics.

Prior to testing, the state of the contact surfaces and initial values of the belt's geometrical values were established. Further measurements were conducted after a certain operation time and are shown in Table 2.

Table 2. Time intervals of measurement of roughness parameters and the belt's geometrical values

Number of measurement	1	2	3	4	5	6	7	8	9	10
Operation time [h]	0	5	10	20	50	100	150	200	250	300

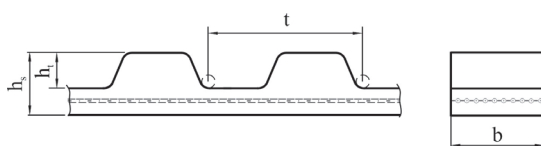


Fig. 5. Measured geometrical values of the belt

### 3 VARIATION OF BELT'S PITCH

Measurement of geometrical values of timing belts was conducted on eight belt's teeth. The following values were measured (Fig. 4) [27]:

1. belt's pitch ( $t$ ),
2. belt's width ( $b$ ),
3. belt groove's thickness ( $h_b = h_s - h_t$ ) and
4. belt's total height ( $h_s$ ).

Belt's pitch is a distance between centres of two consecutive teeth and is measured on the so-called pitch line. Considering the design realization of the belt and the available apparatus, the belt's pitch is measured at the tooth's root. Belt's pitch is determined with the rollers. Namely, the rollers having corresponding radii are set at the roots of the two successive belt's teeth (Fig. 5). Then, the belt with the rollers is set on the auxiliary tool. The tension force exerted on the belt is the same for all measurements. The total length of the belt is determined based on the belt's pitch and the number of teeth. Measurement is

conducted on optical microscope ZEISS ZKM01-250C.

Belt's pitch variation ( $\Delta t$ ) may be shown with the help of the following Eq.:

$$\Delta t = t - t_o, \quad (3)$$

where:  $t$  is the measured value of belt's pitch during testing and  $t_o$  is the initial value of belt's pitch.

Measurement results of belt's pitch variation during the operation for all eight teeth are given in Table 3 and shown in Fig. 6.

Table 3. Belt's pitch variation  $\Delta t = t - t_o$  [ $\mu\text{m}$ ]

Time of operation [h]	$\Delta t$							
	Belt's tooth							
	1	2	3	4	5	6	7	8
5	123	121	121	118	121	118	121	119
10	123	122	121	119	120	118	121	119
20	135	133	133	129	131	129	131	130
50	152	152	151	148	150	147	151	150
100	170	169	167	163	167	166	168	166
150	175	174	173	170	172	170	174	173
200	185	184	184	181	182	178	183	182
250	204	197	197	196	205	196	201	198
300	205	202	207	208	210	198	211	200

In addition, the belt's length is obtained with the help of centre distance, by mounting of the same belt on the two belt pulleys having transmission ratio of 1, with no previous tension. Values of the belt's length determined in both ways were approximately equal, before the belt was tested.

### 4 ANALYSIS OF TRIBOLOGICAL PROCESSES

In the period of running in, there is a sudden increase of belt's pitch. This increase originates from plastic deformation of the belt's tractive element and from the wear of teeth's flanks. Wear by roll-formation (a special form of elastomeric wear) is especially emphasized there and the consequences are a removal of material from the belt's teeth and an increase of pitch [28].

In the period of normal wear, which appears after 20 hours of operation, variation of geometrical values is still strong. After 20 hours of operation, the belt's pitch is still increasing. Variation of the belt's pitch is more pronounced

in the period from 20 to 50 hours of operation, after which it becomes approximately linear. The results obtained by measurement on all the eight teeth almost do not deviate from each other.

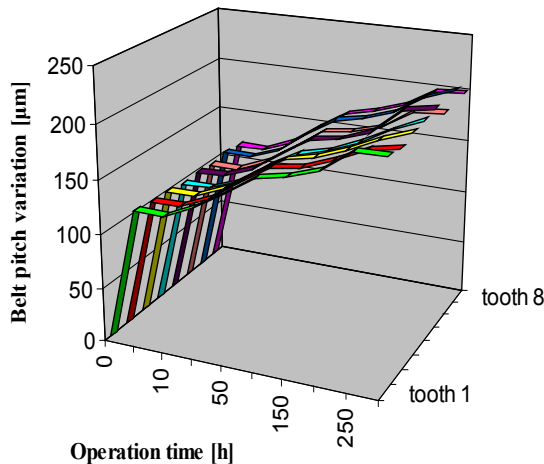


Fig. 6. Belt's pitch variation during exploitation

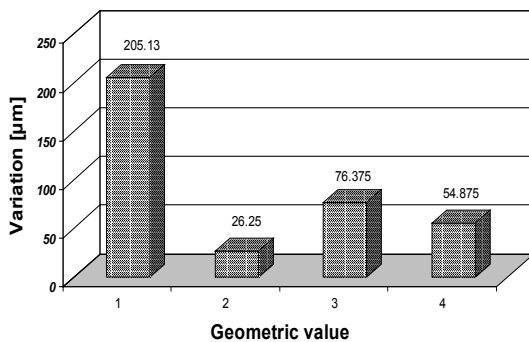


Fig. 7. Average values of variations of geometric values; 1 - Belt's pitch, 2 - Belt's width, 3 - Belt's total height, 4 - Belt groove's thickness

Absolute average values of variation of geometrical values are presented in Fig. 7.

The histogram shows that the belt's pitch changes the most. The belt's pitch increases for approximately 0.2 mm, which leads to an increase of the belt's length. Total elongation of the belt is approximately 23 mm. An increase of the belt's pitch induces variations in kinematics of coupling, reduction of contact surface, increase of friction and the need for additional tightening.

Variation of the belt's pitch arising in the period of running in is a direct consequence of

elongation of the tractive element, i. e. elongation of the belt. Thereat, the tractive element was permanently elongated. Elongation of the belt's pitch is the largest in the period of running (Table 2) and amounts 60% of total elongation. After the period of running in, during the period of normal wear, the belt's pitch was still increasing. The variation of the belt's pitch has almost linear form and it changes continuously until the end of the test. At the same time, the total length of the belt changes very little, i.e. the total variation of the belt's pitch is considerably larger than the variation of the belt's length. A newly created variation of pitch arises, in the first place, due to wear of the flanks of the teeth.

## 5 CONCLUSIONS

An increase of the belt's pitch arises due to plastic deformations of the belt's tractive element and wear by roll-formation of teeth's flanks. An increase of length (elongation) of the tractive element gradually occurs during exploitation and stays permanently, even after the belt is unloaded. A large portion of this increase, approximately 70%, occurs due to plastic deformation of the belt, while the rest of it is due to wear by roll-formation of the belt teeth's flanks. Participation of wear by roll-formation in total elongation of the belt increases with the increase of timing belt's operation time as plastic deformation is the greatest in the period of running in. Variation of the belt's pitch leads to disturbance in operation of timing belt as there are changes in load distribution, reduction of carrying capacity and unevenness in operation. There is a need for additional tensioning of the belt, which directly affects the service life of the drive.

## 6 REFERENCES

- [1] Case, Y.R. (1954). *Timing belt drive*. McGraw Hill Book Company, Inc., New York.
- [2] Stojanovic, B. (2007). *Characteristics of tribological processes in timing belts*. Master's thesis, Faculty of Mechanical Engineering from Kragujevac, Kragujevac. (in Serbian)
- [3] Stojanovic, B., Miloradovic, N. (2009). Development of timing belt drives. *Mobility*



- and *Vehicle Mechanics*, vol. 35, no. 2, p. 31-36.
- [4] Gerbert, G., Jönsson, H., Persson, U., Stensson, G. (1978). Load distribution in timing belts. *Transactions of the ASME, Journal of Mechanical Design*, vol. 100, p. 208-215.
  - [5] Kagotani, M., Koyama, T., Hiroyuki, U., Aida, T., Hoshiro, T. (1984). Load distribution on toothed belt drives under a state of initial tension. *Bulletin of the Japan Society of Mechanical Engineers*, vol. 27, no. 230, p. 1780-1787.
  - [6] Metzner, D., Urbansky, N. (1984). Vorspannkraft bei zahnrriemengetrieben. *Maschinenbautechnik*, vol. 33, p. 559-563.
  - [7] Naji, M.R., Marshek, K.M. (1983). Toothed belt load distribution. *Transactions of the ASME, Journal of Mechanisms*, vol. 105, p. 339-347.
  - [8] Kido, R., Kusano, T., Fujii, T. (1995). Finite element analysis for distribution of toothed belts in two axes drive system. *Transactions of the Japan Society of Mechanical Engineers*, vol. 61, p. 130-136. (in Japanese)
  - [9] Karolev, N.A., Gold, P.W. (1995). Load distribution of timing belt drives transmitting variable torque. *Mechanism and Machine Theory*, vol. 30, no. 4, p. 553-567.
  - [10] Dalgarno, K.W., Day, A.J., Childs, T.H.C. (1993). Finite element analysis of synchronous belt tooth failure. *Proceedings of the Institution of Mechanical Engineers, Part D, Journal of Automobile Engineering*, vol. 207, p. 145-153.
  - [11] Dalgarno, K.W., Day, A.J., Childs, T.H.C. (1994). Synchronous belt materials and belt life correlation. *Proceedings of the Institution of Mechanical Engineers, Part D, Journal of Automobile Engineering*, vol. 208, p. 37-48.
  - [12] Childs, T.H.C., Dalgarno, K.W., Hojjati, M.H., Tutt, M.J. (1997). The meshing of timing belt teeth in pulley grooves. *Proceedings of the Institution of Mechanical Engineers, Part D, Journal of Automobile Engineering*, vol. 211, p. 205-218.
  - [13] Childs, T.H.C., Hojjati, M.H., Kohno, M., Nakamura, T. (1998). Land friction effects in the meshing of timing belts. *Proceedings of the Institution of Mechanical Engineers, Part J, Journal of Engineering Tribology*, vol. 212, p. 87-100.
  - [14] Childs, T.H.C., Dalgarno, K.W., Day, A.J., Moore R.B. (1998). Automotive timing belt life laws and a user design guide. *Proceedings of the Institution of Mechanical Engineers, Part D, Journal of Automobile Engineering*, vol. 212, p. 409-419.
  - [15] Dalgarno, K.W., Day, A.J., Childs, T.H.C., Moore, R.B. (1998). Stiffness loss of synchronous belts. *Composites, Part B: Engineering*, vol. 29, p. 217-222.
  - [16] Johannesson, T., Distner, M. (1999). Model for tooth belt mechanics. *Proceedings of 4<sup>th</sup> World Congress on Gearing and Power Transmission*, Paris, p. 1357-1369.
  - [17] Johannesson, T., Distner, M. (2002). Dynamic loading of synchronous belts. *Transactions of the ASME, Journal of Mechanical Design*, vol. 124, p. 79-85.
  - [18] Callegari, M., Cannella, F. (2001). Lumped-parameter model of timing belt transmissions. *Proceedings of 15<sup>th</sup> AIMETA Congress of Theoretical and Applied Mechanics*, Taormina, p. 1-11.
  - [19] Callegari, M., Cannella, F., Ferri, G. (2003). Multi-body modelling of timing belt dynamics. *Proceedings of the Institution of Mechanical Engineers, Part K: Journal of Multi-body Dynamics*, vol. 217, p. 63-75.
  - [20] Kagotani, M., Ueda, H., Koyama, T. (2001). Transmission error in helical timing belt drives (case of a period of pulley pitch). *Transactions of the ASME, Journal of Mechanical Design*, vol. 123, p. 104-110.
  - [21] Zupancic, B., Nikonov, A., Florjancic, U., Emri, I. (2007). Time-dependent behavior of drive belts under periodic mechanical loading – an analysis of the location of a single line spectrum. *Strojniški vestnik - Journal of mechanical Engineering*, vol. 53, no. 10, p. 696-705.
  - [22] Sheng, G., Zheng, H., Qatu, M., Dukkipati, R.V. (2008). Modelling of friction-induced noise of timing belt. *International Journal of Vehicle Noise and Vibration*, vol. 4, no. 4, p. 285-303.
  - [23] Ueda, H., Kagotani, M., Koyama, T., Nishioka, M. (1999). Noise and life of helical timing belt drives. *Transactions of the ASME*,

- Journal of Mechanical Design*, vol. 121, no. 2, p. 274-279.
- [24] Stojanovic, B., Tanasijevic, S., Miloradovic, N. (2009). Tribomechanical systems in timing belt drives. *Journal of the Balkan Tribological Association*, vol. 15, no. 4, p. 465-473.
- [25] Vorobjev, I.I. (1979). *Belt Drives*. Machine building, Moscow. (in Russian)
- [26] Stojanović, B., Miloradović, N., Blagojević, M. (2009). Analysis of tribological processes at timing belt's tooth flank. *Tribology in Industry*, vol. 31, no. 3-4, p. 53-58.
- [27] ISO 5296-1 (1989). *Synchronous belt drives -- Belts - Part 1: Pitch codes MXL, XL, L, H, XH and XXH - Metric and inch dimensions*. Geneva, International Organization for Standardization.
- [28] Aharoni, S.M. (1973). Wear of polymers by roll-formation. *Wear*, vol. 25, no. 3, p. 309-327.